*33rd EPS Conference on Plasma Phys. Rome, 19 - 23 June 2006 ECA Vol.**30I**, O-4.007 (2006)*

Efficient attosecond phenomena in the relativistic regime

N. M. Naumova[1,2], J. A. Nees[2], I. V. Sokolov[3], E. P. Power[2],
V. P. Yanovsky[2], A. Maksimchuk[2], and G. A. Mourou[1,2]

[1] *Laboratoire d'Optique Appliquee, UMR 7639 ENSTA, Ecole Polytechnique, CNRS, Palaiseau, France*

[2] *Center for Ultrafast Optical Science, University of Michigan, Ann Arbor, MI, USA*

[3] *Space Physics Research Laboratory, University of Michigan, Ann Arbor, MI, USA*

Attosecond electromagnetic pulses and electron bunches, if they can be produced efficiently, can give access to extreme field physics and coherent interaction in x-ray range. We find a path to the efficient generation of strong attosecond electromagnetic pulses and dense attosecond electron bunches in the same domain where conventional lasers themselves are naturally efficient, the regime of tightly focused ultrashort pulses. By focusing few-cycle laser pulses to a diffraction limited spot (the λ^3 regime) relativistic intensity can be achieved even with millijoule energies [1]. In this way using joule-level pulses, an intensity of 10^{22} W/cm^2 has now been demonstrated [2]. As a consequence maximal temporal and spatial gradients are produced in the driving pulse. Applying these gradients to near-critical or over-critical plasma targets ($\omega_0 \leq \omega_{pe}$), particle-in-cell (PIC) simulations show the production of sub-cycle structures of electromagnetic radiation and spiked electron density distributions emerging efficiently from the interaction [3-7].

Interaction of laser pulses with overdense plasmas has been extensively studied theoretically and experimentally [8] and a framework for attosecond pulses has also been established around experiments on harmonic generation from solids [9]. Recently, at the rear side of solid targets evidence of sub-cycle electron bunching was registered with optical transition radiation [10], also implying attosecond phenomena. Interpretation of these observations was done with 1-D models. An oscillating mirror model [11], explaining harmonic generation from relativistically driven overdense plasmas, was developed for plane-wave incidence. Based on that model at normal incidence, a suggestion was made to generate attosecond pulse trains in the reflection of intense laser pulses from solid targets [12]. The bunching of electrons was assigned to either vacuum or $v \times B$ heating mechanisms [8], which are also based on a 1D approach combined with the action of the electric and magnetic parts in the Lorentz force on electrons.

In reality a laser pulse with a finite focal spot cannot possess plane-wave behavior. A range of incidence angles appear along the interaction surface because of the transverse gradient of the pulse. In addition, significant excursions of relativistic electrons lead to modification of the effective interaction surface contour. In the relativistic λ^3 regime, where light is concentrated at focus to a few λ^3 volume, this leads to reflection of the radiation with deflection and compression, providing the generation of isolated attosecond pulses [3-5]. At large angles of incidence dense attosecond electron bunches emerge efficiently from the plasma target into vacuum [5,6]. These two effects observed in PIC simulations demonstrate the highly nonlinear and at least 2D nature of laser-plasma interaction in this regime.

Study of linearly polarized 5-fs (~2 cycles for λ=0.8μm) laser pulses focused to a 1-λ diameter spot with a dimensionless amplitude at focus of $a_0 = eE_0/m\omega_0 c = 3$, interacting with a plasma layer of density $n_0=1.5n_{cr}$ (where $n_{cr}=m_e\omega_0^2/4\pi e^2$), reveals that isolated attosecond pulses are formed with ~10% efficiently [3,4]. As shown in the plot of electromagnetic energy density [Fig. 1(a)], radiation emerging from the target is deflected into different directions. We find three prominent attosecond pulses, among them the most intense (3) is deflected at a larger (non-specular) angle. The strongest pulse is isolated [Fig. 1(b)], and it contains ~10% of the input optical pulse energy within its 50% intensity contour. Electron density plots [Fig. 1(c)] are shown at the instants when compression occurs for each of the three pulses. Electrons moving coherently with relativistic velocities in thin sheets toward the reflected radiation form the attosecond pulses via reflection and Doppler compression. Collecting the radiation with an antenna at points along the maximal value path [Fig. 1(d)] we find that the strongest pulse has a 200-as duration. The power spectrum of this radiation [Fig. 1(e)] has a broadband structure with 96% and 99% of its energy at frequencies respectively below the 4th and 6th harmonics of the driving field, but does not show peaks directly on the harmonics of the incident radiation.

In the interaction of 5-fs cosine-like laser pulses (for which the envelope maximum and the electric field maximum coincide) with plasmas, isolated attosecond pulses are formed efficiently for step-like plasma profiles whose densities scale with a_0 and for exponential plasma profiles with 1-λ gradient scale-length [5]. In 2D simulations the ratio $a_0/n_0=2$ is optimal for the generation of isolated attosecond pulses. Keeping this ratio for 1D simulations in a boosted frame, which allows for oblique incidence, we find that the generated attosecond pulse duration scales as $1/a_0$ with increasing field strength. In the same case, the spectra of attosecond pulses have broader frequency content, allowing for their greater focusability.

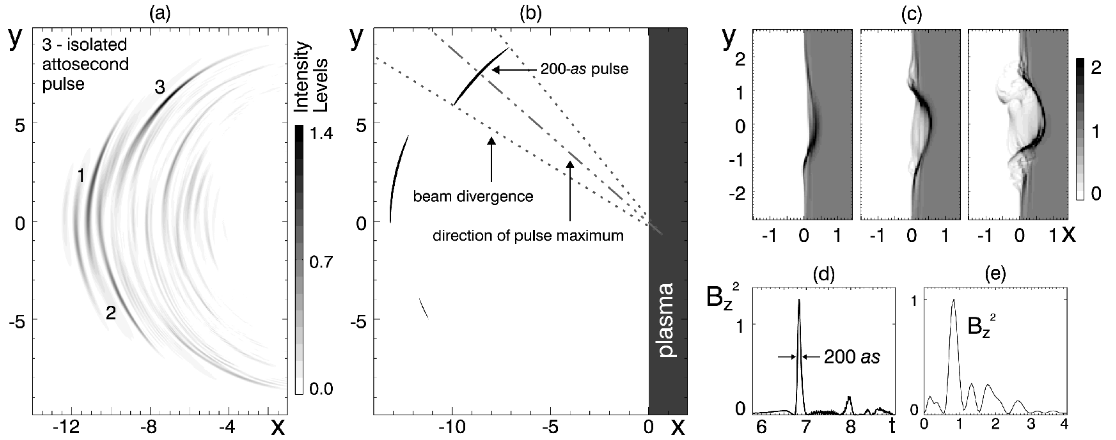

Fig. 1. Generation of attosecond electromagnetic pulses in a 2D PIC simulation. (a) The electromagnetic energy density of the reflected radiation ($W=E^2+B^2$) at t=11. Numbers 1, 2, and 3 indicate the most intense pulses in the reflected radiation: 3 - with the highest intensity, 2 - with the lowest intensity. (b) Half-intensity level of the reflected radiation at t=13. The arrow indicates a single attosecond pulse. (c) Snapshots of the electron density at instants t=-0.5, 0.2, 0.9 when attosecond pulses are formed. (d) The time evolution of B_z^2 at the point x=-3.5, y=3. The arrows indicate the half-intensity level of an isolated pulse that contains 10% of the incident pulse energy. (e) Power spectrum [in arbitrary units] of the magnetic field B_z versus frequency ω/ω_0. Simulation parameters: a_0=3, τ=5 fs, $n_0=1.5n_{cr}$.

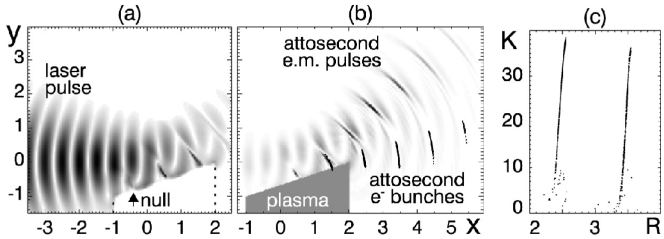

Fig. 2. Trains of attosecond electron bunches and attosecond electromagnetic pulses formed at oblique incidence (70^o) on a short target. Electromagnetic energy density (grey scale): (a) $W^{1/2}$ at t=-3 and (b) W at t=3. In (a) the arrow indicates an electromagnetic field null and in (b) overlapped black dots indicate 25-30 MeV electrons. (c) Kinetic energy (in MeV) of bunched electrons in an arc-projection at t=3. Simulation parameters: a_0=10, τ=15fs, $n_0=25n_{cr}$.

Analyzing the details of laser-plasma interaction in the λ^3 regime, we can also identify conditions under which dense attosecond electron bunches are driven into vacuum [5,6]. This effect we demonstrate with 15-fs linearly polarized laser pulse interacting with a plasma target at an incidence angle 70^o [Fig. 2]. The pulse is focused to a 1-λ diameter spot and has an amplitude a_0=10 at focus. The laser pulse, enhancing the pressure on the plasma target by the sum of the incident and reflected radiation, pushes plasma electrons from the skin layer into the plasma [Fig. 2(a)]. At the same time counterstreaming of electrons occurs. Some counterstreaming electrons escape the plasma through nulls in the electromagnetic field. Being ejected from the plasma with relativistic velocities, these electrons are additionally accelerated by the resulting electromagnetic field, simultaneously compressing the radiation and forming attosecond pulses [Fig. 2(b)]. Thus, the generation of attosecond electron bunches is synchronized with attosecond electromagnetic pulses due to their cooperative nature. Escaping the target, attosecond electron bunches inherit their peaked density distribution. These bunches have chirped energy distribution [Fig. 2(c)] and contain ~10^8 electrons for the indicated laser-plasma parameters. The chirped energy distribution might be exploited to obtain high up-conversion scattering efficiency from a lower charge density.

If the phenomena discussed above are realized experimentally, they offer the potential for the generation of extreme fields and efficient attosecond x-ray generation. The efficiency derived from working with overdense plasmas in the relativistic λ^3 regime enables relativistic attosecond microelectronics.

1. G. Mourou, Z. Chang, A. Maksimchuk, J. Nees, S. V. Bulanov, V. Yu. Bychenkov, T. Zh. Esirkepov, N. M. Naumova, F. Pegoraro, and H. Ruhl, Plasma Phys. Rep. **28**, 12 (2002).
2. S. Bahk, P. Rousseau, T. Planchon, V. Chvykov, G. Kalintchenko, A. Maksimchuk, G. Mourou, and V. Yanovsky, Opt. Lett. **29**, 2837 (2004).
3. N. M. Naumova, J. A. Nees, I. V. Sokolov, B. Hou, and G. A. Mourou, Phys. Rev. Lett. **92**, 063902 (2004).
4. N. M. Naumova, J. A. Nees, B. Hou, G. A. Mourou, and I. V. Sokolov, Opt. Lett. **29**, 778 (2004).
5. J. A. Nees, N. M. Naumova, E. P. Power, V. P. Yanovsky, I. V. Sokolov, A. Maksimchuk, S-W. Bahk, V. Chvykov, G. Kalintchenko, B. Hou, and G. A. Mourou, J. Mod. Optics **52**, 305 (2004).
6. N. Naumova, I. Sokolov, J. Nees, A. Maksimchuk, V. Yanovsky, and G. A. Mourou, Phys. Rev. Lett. **93**, 195003 (2004).
7. N. M. Naumova, J. A. Nees, and G. A. Mourou, Phys. Plasmas **12**, 056707 (2005).
8. S.C. Wilks and W.L. Kruer, IEEE J. Quantum Electr. **33**, 1954 (1997), and references therein.
9. R.L. Carman, C.K. Rhodes, and R.F. Benjamin, Phys. Rev. A **24**, 2649 (1981); S. Kohlweyer, G. D. Tsakiris, C.-G. Wahlström, C. Tillman, and I. Mercer, Opt. Commun. **117**, 431 (1995); D. von der Linde, T. Engers, G. Jenke, P. Agostini, G. Grillon, E. Nibbering, A. Mysyrowicz, and A. Antonetti, Phys. Rev. A **52**, R25 (1995).
10. S. Baton, J. Santos, F. Amiranoff, H. Popescu, L. Gremillet, M. Koenig, E. Martinolli, O. Guilbaud, C. Rousseaux, M. Rabec Le Gloahec, T. Hall, D. Batani, E. Perelli, F. Scianitti, and T. Cowan, Phys. Rev. Lett. **91**, 105001 (2003).
11. S. V. Bulanov, N. M. Naumova, and F. Pegoraro, Phys. Plasmas **1**, 745 (1994); R. Lihters, J. M. ter Vehn, and Pukhov, Phys. Plasmas **3**, 3425 (1996).
12. L. Plaja, L. Roso, K. Rzazewski, and M. Lewenstein, J. Opt. Soc. Am. B **15**, 1904 (1998).